Vapor Infiltration of a Reducing Agent for Facile Synthesis of Mesoporous Pt and Pt-Based Alloys and Its Application for the Preparation of Mesoporous Pt Microrods in Anodic Porous Membranes†

Yusuke Yamauchi,*,‡,§ Azusa Takai,⊥ Masaki Komatsu,⊥ Makoto Sawada,⊥ Tetsu Ohsuna,§,# and Kazuyuki Kuroda*,§,⊥,#

International Center for Materials Nanoarchitectonics, National Institute for Materials Science, Namiki 1-1, Tsukuba, Ibaraki 305-0044, Japan, Kagami Memorial Laboratory for Materials Science and Technology, Waseda University, Nishi-waseda 2-8-26, Shinjuku-ku, Tokyo 169-0051, Japan, Department of Applied Chemistry, Faculty of Science & Engineering, Waseda University, Ohkubo 3-4-1, Shinjuku-ku, Tokyo 169-8555, Japan, and CREST, Japan Science and Technology Agency, Honcho 4-1-8, Kawaguchi-shi, Saitama 332-0012, Japan

Received July 24, 2007. Revised Manuscript Received November 8, 2007

Highly ordered mesoporous Pt and Pt-based alloy (Pt−Ru and Pt−Ni) microparticles were deposited from lyotropic liquid crystal (LLC) films containing corresponding metal species via vapor infiltration of a reducing agent of dimethylaminoborane (DMAB). The LLC films with 2D hexagonal symmetry were prepared on flat substrates from diluted surfactant solutions including water, nonionic surfactant, ethanol, and metal species by drop-coating. Low-angle XRD measurements and TEM observations proved that the deposited Pt and Pt-based alloy microparticles have 2D hexagonally ordered mesoporous structures. Moreover, EDS mapping of mesoporous Pt−Ru microparticles indicated that the constituent metals are well-distributed within the mesopore walls. Moreover, we effectively utilized the method to fabricate mesoporous Pt microrods with 100 nm in diameter by using a porous anodic alumina membrane (PAAM) as a hard template. The Pt microrods possess a highly porous nanostructure. Our method utilizing vapor infiltration of a reducing agent, unlike conventional electrochemical and chemical deposition methods, allows the facile preparation of mesoporous metal microparticles and microrods and should be widely applicable to the deposition of various metals and multicomponent alloys.

Introduction

Since the discovery of mesoporous silica (KSW-1) from kanemite in 1990,[1] ordered mesoporous materials have attracted a great deal of attention worldwide because of their potential new applications.[2,3] Mesoporous metal-based materials (mesoporous metals) are more useful than coventional silica-based mesoporous materials in the fields of electronic devices, magnetic devices, metal catalysts, etc. Since the pioneering work on mesoporous Pt particles by Attard et al.,[4] many kinds of mesoporous metals[4–10] and related metal-based nanomaterials[11–14] have been successfully prepared by reducing the corresponding metal species dissolved in aqueous domains of lyotropic liquid crystals (LLC).

The general synthesis of mesoporous metals using LLC is a two-step process: (1) formation of LLC and (2) reduction

† Part of the "Templated Materials Special Issue".

* Corresponding author. E-mail: YAMAUCHI.Yusuke@nims.go.jp (Y.Y.); kuroda@waseda.jp (K.K.).

‡ National Institute of Materials Science.

§ Kagami Memorial Laboratory for Materials Science and Technology, Waseda University.

⊥ Faculty of Science & Engineering, Waseda University.

Japan Science and Technology Agency.

(1) (a) Yanagisawa, T.; Shimizu, T.; Kuroda, K.; Kato, C. *Bull. Chem. Soc. Jpn.* **1990**, *63*, 988–992. (b) Yanagisawa, T.; Shimizu, T.; Kuroda, K.; Kato, C. *Bull. Chem. Soc. Jpn.* **1990**, *63*, 1535–1537. (c) Shimojima, A.; Kuroda, K. *Chem. Rec.* **2006**, *6*, 53–63.

(2) (a) Murakami, M.; Shimizu, T.; Tansho, M.; Vinu, A.; Ariga, K.; Takegoshi, K. *Chem. Lett.* **2006**, *35*, 986–987. (c) Vinu, A.; Srinivasu, P.; Mori, T.; Sasaki, T.; Asthana, A.; Ariga, K.; Hishita, S. *Chem. Lett.* **2007**, *36*, 770–771.

(3) Wan, Y.; Zhang, D.; Zhai, Y.; Feng, C.; Chen, J.; Li, H. *Chem.—Asian J.* **2007**, *2*, 875–881.

(4) Attard, G. S.; Göltner, C. G.; Corker, J. M.; Henke, S.; Templer, R. H. *Angew. Chem., Int. Ed.* **1997**, *36*, 1315–1317.

(5) (a) Attard, G. S.; Bartlett, P. N.; Coleman, N. R. B.; Elliott, J. M.; Owen, J. R.; Wang, J. H. *Science* **1997**, *278*, 838–840. (b) Nelson, P. A.; Elliott, J. M.; Attard, G. S.; Owen, J. R. *Chem. Mater.* **2002**, *14*, 524–529. (c) Elliott, J. M.; Attard, G. S.; Bartlett, P. N.; Coleman, N. R. B.; Merckel, D. A. S.; Owen, J. R. *Chem. Mater.* **1999**, *11*, 3602–3609. (d) Attard, G. S.; Leclerc, S. A. A.; Maniquet, S.; Russell, A. E.; Nandhakumar, I.; Bartlett, P. N. *Chem. Mater.* **2001**, *13*, 1444–1446. (e) Markham, M. L.; Baumberg, J. J.; Smith, D. C.; Li, X.; Gabriel, T.; Attard, G. S.; Nandhakumar, I. *Appl. Phys. Lett.* **2005**, *86*, 011912.

(6) Luo, H. M.; Sun, L.; Lu, Y. F.; Yan, Y. S. *Langmuir* **2004**, *20*, 10218–10222.

(7) Boo, H.; Park, S.; Ku, B. Y.; Kim, Y.; Park, J. H.; Kim, H. C.; Chung, T. D. *J. Am. Chem. Soc.* **2004**, *126*, 4524–4525.

(8) (a) Jiang, J.; Kucernak, A. *J. Electroanal. Chem.* **2002**, *520*, 64–70. (b) Jiang, J.; Kucernak, A. *J. Electroanal. Chem.* **2002**, *533*, 153–165. (c) Kucernak, A.; Jiang, J. *Chem. Eng. J.* **2003**, *93*, 81–91. (d) Jiang, J. H.; Kucernak, A. *J. Electroanal. Chem.* **2003**, *543*, 187–199. (e) Jiang, J. H.; Kucernak, A. *Chem. Mater.* **2004**, *16*, 1362–1367.

(9) Planes, G. A.; Garcia, G.; Pastor, E. *Electrochem. Commun.* **2007**, *9*, 839–844.

(10) (a) Yamauchi, Y.; Yokoshima, T.; Momma, T.; Osaka, T.; Kuroda, K. *Chem. Lett.* **2004**, *33*, 1576–1577. (b) Yamauchi, Y.; Momma, T.; Fuziwara, M.; Sivakumar Nair, S.; Ohsuna, T.; Terasaki, O.; Osaka, T.; Kuroda, K. *Chem. Mater.* **2005**, *17*, 6342–6348.

10.1021/cm701985f CCC: $40.75
Published on Web 12/12/2007

of metal ions in the presence of LLC.[4–10] In the first stage, a large amount of surfactant is necessary to form LLC, which consists of highly concentrated surfactants (normally more than 40 wt %). Ternary components (including surfactants, water, and metal species) are manually mixed, and the mixture is then heated and mixed vigorously. This process is repeated until a homogeneous mixture is obtained. LLC is thus prepared manually. To avoid the multistep processes, we have recently proposed a formation process of LLC through solvent evaporation (Evaporation-mediated Direct Templating, EDIT).[15] In this method, a LLC templating mixture can be directly formed from a diluted surfactant solution (precursor solution) without heating-aging processes.[4–10] Very recently, Edler et al.[16] and Kijima and Sakai et al.[17] applied this concept to make mesoporous Ag films and nanogroove-network-structured Pt nanosheets, respectively.

In the second stage, some problems still remain. By electrochemical and chemical deposition, mesoporous metals have been generally formed as films on conductive substrate and as powders dispersed in solutions, respectively.[4–10] The electrodeposition using an external power source has been the main method of reducing metal ions. The electrodeposition system involves a three-electrode cell consisting of a working, a reference, and a counter electrode. Mesoporous metal thin films are deposited onto conductive substrates that act as a working electrode. However, it is difficult to set up and operate the three-electrode cell because of the high viscosity of LLC, in contrast to the conventional electrodeposition system of metals using an aqueous solution. Another problem is that the previous systems are limited to deposition onto conductive layers. Therefore, a new simpler and more sophisticated synthetic route is needed. So we aimed to create a procedure of synthesizing highly ordered mesoporous metals and alloys to fulfill the requirements for a wider applicability to any kinds of substrates including nonconductive ones.

In this study, we propose a unique and versatile approach for synthesizing highly ordered mesoporous Pt and Pt-based alloy (Pt−Ru and Pt−Ni) microparticles through vapor infiltration of a reducing agent. LLC films including metal species were spontaneously and directly formed through solvent evaporation from a diluted surfactant solution. The LLC films were then put into a closed container together with a reducing agent, and mesoporous metal microparticles were deposited in the presence of LLC through vapor infiltration of the reducing agent. Vapor infiltration of reducing agents for the preparation of metal nanoparticles has been reported,[18–20] but there are no reports to apply this method for the preparation of mesoporous metals. Our approach reported here, unlike the above conventional electrochemical/chemical deposition methods, is an easy way to prepare mesoporous metals and can be used to deposit various metals and multicomponent alloys microparticles over the entire area of substrates without external power sources. Furthermore, the most important point is that our method is highly useful for direct deposition of mesoporous metals onto nonconductive substrate in confined spaces (i.e., anodic porous membranes, micropatterned channels by a lithography technique, etc.). As the first stage, here we report the method to fabricate mesoporous Pt microrods with 100 nm in diameter by using a porous anodic alumina membrane (PAAM) as a hard template, and this should be an important finding for facile control of shapes and morphologies of mesoporous metals.

Scheme 1. Schematic View of Experimental Procedure for Preparing of Mesoporous Pt Microparticles

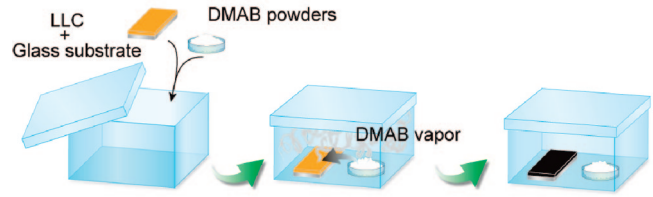

Experimental Section

Materials. Nonionic surfactant ($C_{16}H_{33}(OCH_2CH_2)_8OH$, $C_{16}EO_8$, Aldrich) was used to form lyotropic liquid crystals. Hydrogen hexachloroplatinate (IV) hexahydrate ($H_2PtCl_6 \cdot 6H_2O$ > 98%, Kanto Kagaku Co.), ruthenium (III) trichloride ($RuCl_3$ > 99%, Aldrich), and nickel chloride (purity >98%, Junsei Chemical Co.) were used as Pt, Ru, and Ni sources, respectively. Ethanol (H_2O content <0.005%, Junsei Chemical Co.) was used for both dilution of precursors and removal of templates.

Synthesis of Mesoporous Pt and Pt-Based Alloy Microparticles. The experimental procedure is schematically shown in Scheme 1. First, lyotropic liquid crystal (LLC) films were prepared by drop-coating. Glass substrates were cut into pieces (5 cm × 5 cm) and were used as substrates. A precursor solution (diluted surfactant solution) for mesoporous Pt microparticles was prepared by mixing 0.145 g of distilled water, 0.21 g of nonionic surfactant $C_{16}EO_8$, 0.145 g Pt species, and 0.23 mL of ethanol as a volatile solvent. The precursor solution was then drop-coated onto a glass substrate. After the volatile solvent was preferentially evaporated, an LLC film including Pt species was formed over the entire substrate. The thickness of the LLC film is about 0.5 mm. The resulting LLC film was placed in a closed vessel (380 mL) with a small amount of dimethylaminoborane (DMAB) in a dish, and the

(11) (a) Braun, P. V.; Osenar, P.; Stupp, S. I. *Nature* **1996**, *380*, 325–328. (b) Braun, P. V.; Osenar, P.; Tohver, V.; Kennedy, S. B.; Stupp, S. I. *J. Am. Chem. Soc.* **1999**, *121*, 7302–7309. (c) Braun, P. V.; Osenar, P.; Twardowski, M.; Tew, G. N.; Stupp, S. I. *Adv. Funct. Mater.* **2005**, *15*, 1745–1750.
(12) (a) Kijima, T.; Yoshimura, T.; Uota, M.; Ikeda, T.; Fujikawa, D.; Mouri, S.; Uoyama, S. *Angew. Chem., Int. Ed.* **2003**, *43*, 228–232. (b) Fujikawa, D.; Uota, M.; Yoshimura, T.; Sakai, G.; Kijima, T. *Chem. Lett.* **2006**, *35*, 432–433.
(13) Herricks, T.; Chen, J.; Xia, Y. *Nano Lett.* **2004**, *4*, 2367–2371.
(14) Ganesh, V.; Lakshminarayanan, V. *Langmuir* **2006**, *22*, 1561–1570.
(15) (a) Yamauchi, Y.; Momma, T.; Osaka, T.; Kuroda, K. Japanese Patent 2006-233272. (b) Yamauchi, Y.; Momma, T.; Kitoh, H.; Osaka, T.; Kuroda, K. *Electrochem. Commun.* **2005**, *7*, 1364–1370. (c) Yamauchi, Y.; Kitoh, H.; Momma, T.; Osaka, T.; Kuroda, K. *Sci. Technol. Adv. Mater.* **2006**, *7*, 438–445. (d) Yamauchi, Y.; Kuroda, K. *Electrochem. Commun.* **2006**, *8*, 1677–1682. (e) Yamauchi, Y.; Ohsuna, T.; Kuroda, K. *Chem. Mater.* **2007**, *19*, 1335. (f) Yamauchi, Y.; Komatsu, M.; Takai, A.; Sebata, R.; Sawada, M.; Momma, T.; Fuziwara, M.; Osaka, T.; Kuroda, K. *Electrochim. Acta* **2007**, *53*, 604–609.
(16) Luo, K.; Walker, C. T.; Edler, K. J. *Adv. Mater.* **2007**, *19*, 1506–1509.
(17) Sakai, G.; Yoshimura, T.; Isohata, S.; Uota, M.; Kawasaki, H.; Kuwahara, T.; Fujikawa, D.; Kijima, T. *Adv. Mater.* **2007**, *19*, 237–240.
(18) Hassan, S. United States Patent Application 20060110528.
(19) Surasit, C.; Craig, D. United States Patent 6207551.

Scheme 2. Schematic View of Experimental Procedure for Preparing of Mesoporous Pt Microrods

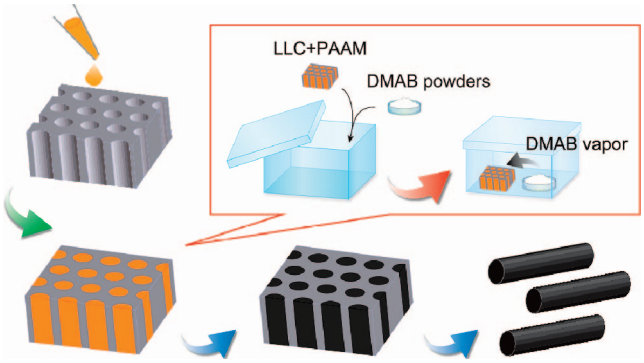

vessel was kept at 25 °C for 15 h. The LLC film was exposed to saturated DMAB vapor under autogenous pressure. During the process, Pt was gradually deposited in the presence of LLC. The film color uniformly changed from orange to black. After Pt deposition, mesoporous Pt microparticles were washed with ethanol and deionized water to remove surfactants.

For the preparation of mesoporous Pt−Ru alloy microparticles, a precursor solution was prepared by mixing 0.145 g of distilled water, 0.21 g of nonionic surfactant $C_{16}EO_8$, 0.105 g of Pt species, 0.0174 g of Ru species, and 0.23 mL of ethanol. The molar ratio of Pt:Ru was 80:20. For the preparation of mesoporous Pt−Ni alloy microparticles, a precursor solution was prepared by mixing 0.145 g of distilled water, 0.21 g of nonionic surfactant $C_{16}EO_8$, 0.0725 g of Pt species, 0.0181 g of Ni species, and 0.23 mL of ethanol. The ratio of Pt:Ni was 50:50.

Preparation of Mesoporous Pt Microrods. The experimental procedure is schematically shown in Scheme 2. For the preparation of mesoporous Pt microrods, the same precursor solution was dropped onto a porous anodic alumina membrane (PAAM) (Pore size, 100 nm, depth, 60 μm) and was simply introduced into channels of PAAM due to a capillary force. LLC was gradually formed within the channels through evaporation of ethanol. Both the PAAM and 0.5 g of DMAB powders as a reducing agent were then put in a closed container and Pt species were reduced by vapor infiltration. After 15 h at 25 °C, PAAM was washed by ethanol to remove surfactants and subsequently PAAM was soaked in an aqueous solution of 5 wt % phosphoric acid to dissolve PAAM.

Characterization. The liquid crystalline state of the templating mixture on a glass substrate was confirmed by an Olympus BX-51 optical microscope under a crossed Nicol field, and images were recorded on a digital camera (Canon IXY DIGITAL 800 IS). The $\theta-2\theta$ scanning profiles in the lower diffraction angles were measured by a Mac Science M03XHF22 diffractometer with Mn-filtered Fe-Kα radiation (40 kV, 20 mA) at a scanning rate of 0.5°/min. The $\theta-2\theta$ scanning profiles in the higher diffraction angles were measured by a RINT-TTR III (50 kV, 300 mA) at a scanning rate of 0.5°/min. TEM images were observed by a JEOL JEM-2010 transmission electron microscope using an accelerating voltage of 200 kV and a JEOL JEM-ARM1250 transmission electron microscope using an accelerating voltage of 1250 kV. High-resolution scanning electron micrographs without any metal coating were observed with a Hitachi S-5500 scanning electron microscope using an accelerating voltage of 30 kV.

Results and Discussion

First, a lyotropic liquid crystal (LLC) film including Pt species through solvent evaporation was fully characterized. The precursor solution consisting of Pt species, nonionic surfactant ($C_{16}EO_8$), water, and ethanol was homogeneous

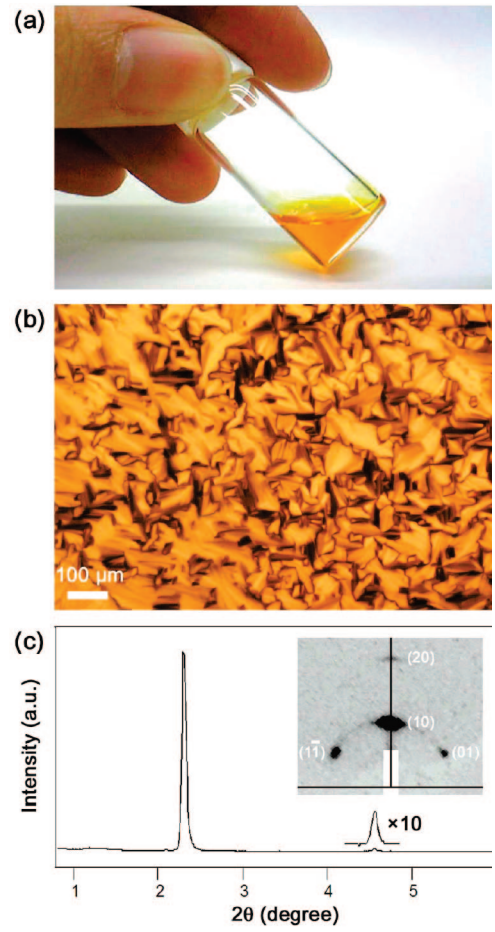

Figure 1. (a) Photograph of a diluted surfactant solution (precursor solution) for preparation of a LLC film including Pt species. The solution is composed of Pt species, surfactant, water, and ethanol. (b) Polarized optical microscopic image of a LLC film including Pt species after solvent evaporation. (c) $\theta-2\theta$ scanning XRD profiles of the LLC film. Inset image is the 2D XRD pattern of the LLC film.

and orange in color and had very low viscosity (Figure 1a). The precursor solution was drop-coated onto a glass substrate. At the initial stage, liquid crystallinity could not be observed at all. As ethanol progressively evaporated, liquid crystallinity appeared and gradually grew, as confirmed by in situ observation. The final LLC after ethanol evaporation showed a typical fanlike texture that is a representative feature of 2D hexagonal (H_I) LLC (Figure 1b).[21] The single domain size of the LLC was estimated to be about 100 μm. A similar phenomenon was observed in the previous case of a LLC film including Pt and Ru species through solvent evaporation.[15e] The low-angle XRD pattern of the formed LLC (Figure 1c) shows two diffraction peaks (d = 4.8 and 2.4 nm) assignable to (10) and (20) planes in a 2D hexagonal ($p6mm$) symmetry with the lattice parameter of 5.5 nm (Figure 1c). The (11) peak could not be observed because the rodlike self-assemblies are formed with the (10) face

(20) Satta, A.; Shamiryan, D.; Baklanov, M. R.; Whelan, C. M.; Le, Q. T.; Beyer, G. P.; Vantomme, A.; Maex, K. *J. Electrochem. Soc.* **2003**, *150*, G300–G306.
(21) (a) Çelik, Ö.; Dag, Ö. *Angew. Chem., Int. Ed.* **2001**, *40*, 3800–3803. (b) Dag, Ö.; Samarskaya, O.; Tura, C.; Gunay, A.; Çelik, Ö. *Langmuir* **2003**, *19*, 3671–3676. (c) Dag, Ö.; Alayoglu, S.; Uysal, I. *J. Phys. Chem. B* **2004**, *108*, 8439–8446.

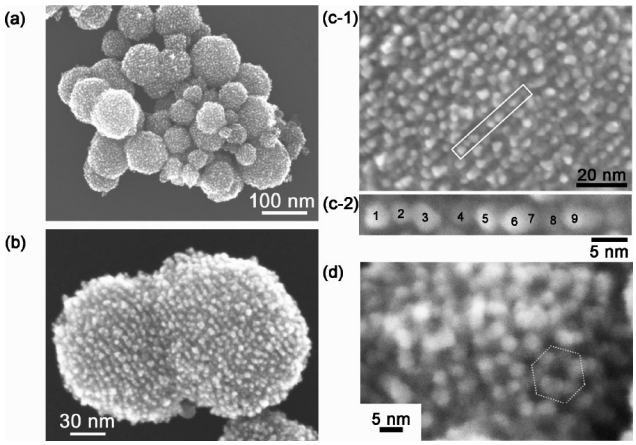

Figure 2. (a) Low-magnification SEM image of mesoporous Pt microparticles. (b) Highly magnified SEM image of the mesoporous Pt microparticles. (c, d) Ultrahigh-magnification SEM images of (c) 1D mesochannels and (d) honeycomb arrangements of mesopores (marked by lines). Figure c-2 is an enlarged view of the square area in Figure c-1. Connected nanoparticles like a necklace are clearly highlighted.

aligned parallel to the substrate.[22] The 2D XRD pattern also shows three spots assigned to (10), (1–1), and (01) in 2D hexagonal symmetry (Figure 1c, inset).[22a] Consequently, our process through solvent evaporation allows the direct formation of LLC from a precursor solution without general heating-aging processes.

In the present "direct templating" approach, the LLC is directly used as a template to synthesize mesoporous metals, and so the mesostructural ordering of the LLC greatly affects those of deposited mesoporous metals.[4,5a,10a] Hence, high-quality LLC films must be used as a starting material, and their stability during Pt deposition for 15 h is an important factor. Thus, we investigated the stability of the LLC containing Pt species by time-dependent XRD patterns. The LLC formed on a glass substrate was put inside a closed container. Even after 24 h, the XRD pattern of the LLC remained unchanged (not shown), meaning that water molecules do not easily evaporate once the LLC is formed, implying that water molecules are stabilized in the hydrophilic domains of LLC and that LLC retains its well-ordered mesostructure for a long time during Pt deposition. Previously, we prepared a LLC thin film by spin-coating for direct deposition of nanostructured Pt layers into a Ni foam.[15f] The stability of the present LLC film by drop-coating is almost the same as that of the LLC film prepared by spin-coating.[15f]

For the deposition of Pt, the LLC was placed together with dimethylaminoborane (DMAB) as a reducing agent in a closed vessel at 25 °C. After 12 h, the color of the LLC changed from orange to black, indicating the progress of Pt deposition. The SEM image of the deposited Pt after removal of surfactants shows the spherical microparticles ca. 50–200 nm in size (images a and b in Figure 2). From the high-magnification SEM images of the mesoporous Pt microparticles, both uniform arrays of mesochannels (Figure 2c) and

(22) (a) Miyata, H.; Kuroda, K. *Chem. Mater.* **2000**, *12*, 49–54. (b) Yamauchi, Y.; Sawada, M.; Noma, T.; Ito, H.; Furumi, S.; Sakka, Y.; Kuroda, K. *J. Mater. Chem.* **2005**, *15*, 1137–1140. (c) Fukumoto, H.; Nagano, S.; Seki, T. *Chem. Lett.* **2006**, *35*, 180–181.

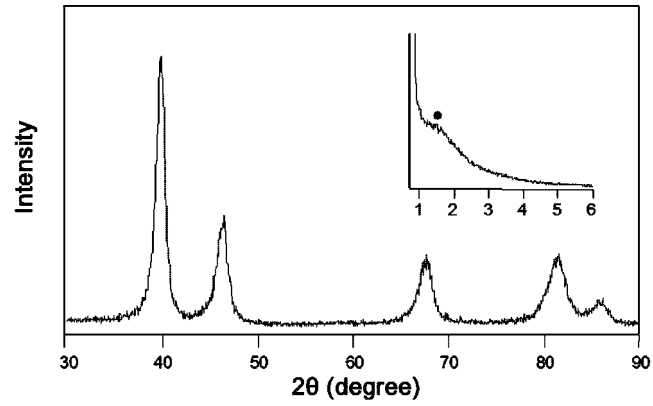

Figure 3. Powder XRD pattern (Cu Kα) of mesoporous Pt microparticles. Inset: XRD pattern (Fe Kα) in the low-angle range.

honeycomb arrangements of mesopores (Figure 2d) were directly observed on the external surface of each microsphere. The mesopore walls are composed of connected nanoparticles with an average size of about 3 nm (Figure 2c-2). We observed a similar phenomenon for mesoporous Pt prepared by chemical reduction using Zn powders[10b] and explained the formation of connected nanoparticles by the mechanism of nanoscale metal deposition in the presence of LLC.[10b,15e] The Pt microparticles were scratched from the substrate, and the low-angle XRD pattern of the powdery sample was measured (Figure 3, inset). A single broad diffraction peak was observed in the range of $1° < 2\theta < 2°$. The broad diffraction in the low-angle XRD pattern is in clear contrast to the ordered regular mesostructure observed in the SEM image (Figure 2). In our previous report, we have already discussed about the reason why the low-angle peak is broadened.[10b] The specific surface area was calculated to be 70 m^2/g (BET) from N_2 adsorption data. The literature values for the specific surface area of platinized Pt films and Pt black powders are 2−30 and 20−26 m^2/g, respectively. In the previous reports, the surface areas of 2D hexagonally ordered mesoporous Pt films and particles prepared from LLC with the same surfactants ($C_{16}EO_8$) range from 17 to 65 m^2/g.[4,5e,8,10b] Also, those of mesoporous Pt−Ru alloys prepared from LLC with Brij 76 ($C_{18}EO_{10}$) is about 86 m^2/g.[5d] Consequently, the surface areas of about 70 m^2/g obtained in this study is almost comparable to the higher values in the range and can be ascribed to the ordered mesoporous structures.

Figure 4 shows the TEM images of the mesoporous Pt microparticles. Both the pore diameter and the thickness of the pore wall are ca. 3.0 nm (Figure 4a). The pore-pore distance is ca. 6 nm. The *p6mm* symmetry cannot simply be assigned on the basis of these TEM images. However, we can observe only stripes and honeycomb structures on all the observed samples. Any periodicities derived from 3D mesostructures were not observable. Therefore, we can conclude that the obtained mesoporous Pt has a *p6mm* symmetry. The high-magnification TEM images in images b and c in Figure 4 reveal the presence of connected nanoparticles in the framework. One nanoparticle of ca. 3 nm (i.e., on a local scale) can be regarded as "single-crystalline domain". The lattice fringes on one

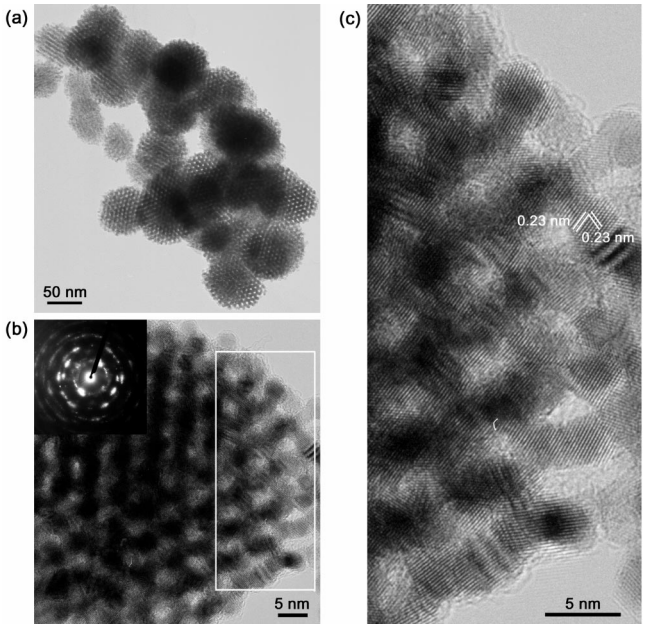

Figure 4. (a) TEM image of typical mesoporous Pt microparticles. (b) High-magnification TEM image with the incident electron beam parallel to the direction of 1D mesochannels. The inset image is electron diffraction pattern of the selected area of 50 nm. (c) Enlarged view of the square area in image b.

nanoparticle correspond to the {111} planes because both *d*-spacings are ca. 0.23 nm and the dihedral angle is ca. 70° (Figure 4c). The selected-area ED pattern from a 50 nm region (i.e., equal to the size of one Pt microparticle shown in Figure 4b) shows ringlike patterns with intense spots assignable to fcc Pt (Figure 4b, inset). The presence of the intense spots indicates that the lattice fringes are coherently running across several nanoparticles to some extent. Additionally, the powder X-ray diffraction profile in the wide-angle (Cu Kα radiation) shows (111), (200), (220), (311), and (222) diffraction peaks assigned to the Pt fcc structure, suggesting that the whole area of the samples has a Pt fcc atomic arrangement (Figure 3).

It should be noted that the arcs are wider than those of mesoporous Pt prepared by chemical reduction using Zn powders in our previous work,[10b] indicating that the atomic crystallinity of the present system is lower. We believe that the degree of atomic crystallinity strongly depends on the deposition behavior of Pt. In the previous system using Zn powders, the Pt deposition was performed with transferred electrons created by dissolving Zn powders, that is, the deposition of the first Pt nanoparticle starts from only the external surface of Zn powders.[10b] The second Pt nanoparticle is then thought to be formed from another nucleus generated on the external surface of the first Pt nanoparticle.[10b] In this way, the connected Pt nanoparticles are deposited continuously, while retaining the single-crystalline-like state to some extent. On the other hand, in the present system, Pt species were reduced by DMAB. The reduction process is suggested to be as follows. DMAB vapor molecules reach the surface of the LLC thin film and dissolve in the hydrophilic region of LLC. DMAB molecules release electrons by self-decomposition reactions, and eventually Pt species are reduced. A large amount of DMAB molecules

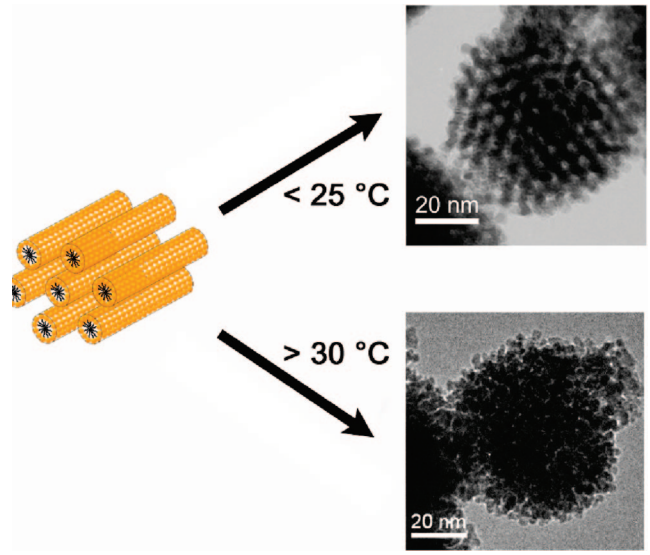

Figure 5. Schematic representation of 2D hexagonal LLC mesophase and TEM images demonstrating the result of different deposition temperatures. (Top) The good templating is achieved when the reaction temperature was lower than 25 °C. (Bottom) Poorly ordered product is obtained when the Pt deposition is carried out at an elevated temperature higher than 30 °C.

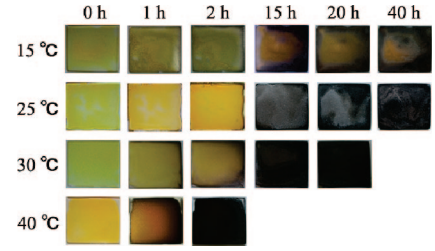

Figure 6. Pt deposition behavior in LLC films under various reaction temperatures.

infiltrate from the upper side of the LLC thin film one after another. The deposition of Pt nanoparticles is thought to occur all over the LLC by the self-decomposition reaction of DMAB. In other words, the nucleation reaction preferentially proceeds rather than the grain growth reaction, which is in contrast to the chemical reduction system using Zn powders. Therefore, the connection of Pt nanoparticles is not performed continuously, meaning that the atomic crystallinity becomes lower compared to that of the Zn system.

The ordering of the mesostructure in deposited Pt microparticles is strongly dependent on the reaction temperature in the closed vessel during the Pt deposition. Highly ordered mesoporous Pt microparticles, shown in Figure 4a, were obtained when the reaction temperature was lower than 25 °C, whereas disordered mesoporous Pt microparticles were obtained at a temperature higher than 30 °C (Figure 5). The time required for the color change from orange to black tended to be shorter (Figure 6), meaning that the deposition rate gradually increased as the reaction temperature was increased. We therefore think that the slow deposition rate is very important to achieve mesoporous metals of the highest quality (Figure 5). In a previous report on the production of a mesoporous Pt film by the electrodeposition method by Attard et al., the slow Pt deposition controlled by the potential was appropriate for attaining a highly ordered

mesostructure.[5c] In our previous work on mesoporous Ni particles by the electroless deposition method, the slow deposition rate of Ni in LLC played a key role for creating highly ordered mesoporous Ni particles.[10a] On the other hand, when the deposition rate of Ni is high under the different kinds of reducing agents, the deposited Ni can not sufficiently coat the rodlike self-assemblies, resulting in the formation of disordered mesoporous Ni.

Additionally, the total yield of the deposited mesoporous Pt is varied by experimental conditions (e.g., reaction temperature, deposition time). The total yield of the highly ordered mesoporous Pt deposited at 25 °C for 15 h (Figures 2 and 4) was about 20%, that is, 80% of the Pt species were undeposited in the LLC film. As the reaction temperature was higher, the total yield was higher. However, low reaction temperature is vital to achieve mesoporous metals of the highest quality (Figure 5). Of course, as the deposition time was longer, the total yield was higher. In the case of mesoporous Pt deposited at 25 °C, the amount of the sample prepared for 20 h is twice as much as that for 15 h. Ordered mesoporous structures are observable by TEM even after such a longer Pt deposition.

In this study, we have chosen DMAB as the most suitable reducing agent from several reducing agents. First, we considered that the solubility of reducing agents into water is an important factor in affording highly ordered mesoporous metals. For example, the volatilities of reducing agents such as trimethylamineborane, sodium borohydride, and sodium hypophosphite acid are very low, compared to DMAB. Therefore, the reduction of metal species in LLC does not proceed even when the temperature was higher than 30 °C. If the temperature is much higher, metal deposition may occur. But, LLC cannot retain the ordered mesostructures under the temperatures higher than 80 °C.[23] Therefore, these reducing agents are not suitable. Second, it is necessary that reducing agents should be easily dissolved into an aqueous phase in LLC, because metal species exist in the aqueous domain of LLC. Formaldehyde is another reducing agent. However, formaldehyde is insoluble in water and causes phase separation with water. Actually, when we used formaldehyde as a reducing agent, the metal deposition can not be observed. As hydrazine was gradually penetrated into the LLC film, the LLC with a 2D hexagonal structure was transformed into a lamella structure, as confirmed by XRD analysis. On the basis of these facts, DMAB was adopted as a reducing agent, being suitable in making mesoporous metals in the present system. DMAB can be easily dissolved into an aqueous domain in LLC and have a sufficient volatility to reduce metal species in LLC under room temperature.

Another significant advantage of the vapor infiltration method is its wide applicability to various mesoporous alloys. As an example, mesoporous Pt−Ru and Pt−Ni alloy microparticles were synthesized by mixing two kinds of metal species, as shown in Figure 7. From the EDS analysis attached to SEM, the composition ratios of the mesoporous

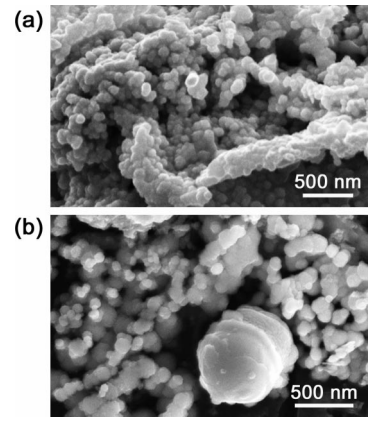

Figure 7. SEM images of (a) mesoporous Pt−Ru alloy and (b) Pt−Ni alloy microparticles.

Pt−Ru and Pt−Ni alloy microparticles were measured to be Pt:Ru = 93:7 and Pt:Ni = 93:7, respectively. The starting composition molar ratios were Pt:Ru = 80:20 and Pt:Ni = 50:50, respectively. Therefore, Pt was preferentially deposited in the presence of LLC because of the difference in the standard electrode potentials (Pt, 1.19 V; Ru, 0.46 V; Ni, −0.26 V).[24]

Figure 8 shows the TEM and EDS mapping images of the obtained mesoporous Pt−Ru and Pt−Ni alloy microparticles. The TEM image shows a highly mesoporous structure consisting of 2D hexagonally arranged mesopores (images a and d in Figure 8). The pore−pore distance is found to be ca. 6 nm, which corresponds to that of the mesoporous Pt microparticles. In the higher magnified TEM image, the framework shows that the pore wall is composed of connected nanoparticles with an average size of ca. 3 nm (Figure 8b). The structures observed here are similar to those of the above mesoporous Pt microparticles (Figure 4a).

Figure 8c shows the EDS mapping of the mesoporous Pt-Ru alloy particles. The dark-field (DF) STEM image corresponds to the images of the EDS mapping of Pt and Ru. The Pt and Ru atoms are homogeneously dispersed. No phase separations in a nanometer scale are observed. The selected-area ED pattern from a 50 nm region shows a ring pattern assigned to the fcc structure (Figure 8b, inset). High-magnification TEM images proved that the lattice fringes are randomly oriented across the connected nanoparticles (Figure 8b). Note that the domain size of a single crystal is smaller than that of mesoporous Pt microparticles (Figure 4c) under the same experimental conditions. We suppose that the codeposition of two metal species having different standard electrode potentials (E_0) may affect the reduction of the domain size of the single atomic crystallinity.[25,26] This phenomenon was also observed in our previous study on preparing mesoporous Pt−Ru alloy by the electrodeposition method.[15e]

(23) Attard, G. S.; Bartlett, P. N.; Coleman, N. R. B.; Elliott, J. M.; Owen, J. R. *Langmuir* **1998**, *14*, 7340–7342.

(24) Milazzo, G., Caroli, S., Eds.; *Tables of Standard Electrode Potentials*; John Wiley & Sons Ltd.: New York, 1978.

(25) Park, K. W.; Choi, J. H.; Kwon, B. K.; Lee, S. A.; Sung, Y. E.; Ha, H. Y.; Hong, S. A.; Kim, H.; Wieckowski, A. *J. Phys. Chem. B* **2002**, *106*, 1869–1877.

(26) Huang, J. C.; Liu, Z. L.; He, C. B.; Gan, L. M. *J. Phys. Chem. B* **2005**, *109*, 16644–16649.

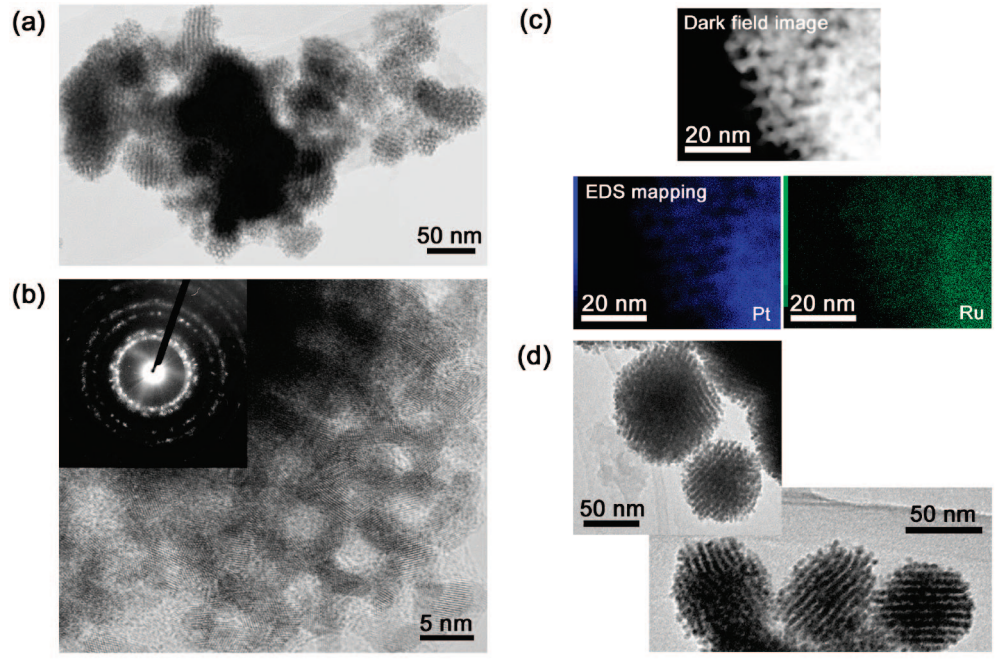

Figure 8. (a) Low-magnification TEM image of mesoporous Pt−Ru alloy microparticles. (b) High-magnification TEM image. Inset image is the selected-area ED pattern in 50 nm range. (c) EDS mapping of mesoporous Pt−Ru alloy particle. Dark-field (DF) image and the elemental distributions of Pt and Ru. (d) Low-magnification TEM image of mesoporous Pt−Ni alloy microparticles.

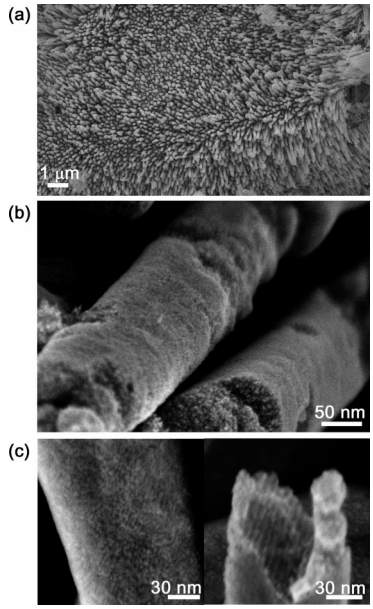

Figure 9. SEM images of mesoporous Pt microrods prepared by PAAM. (a) Low-magnification SEM image. (b) High-magnification SEM images. Spongelike nanostructures are observed within the microrods. (c) High-magnification SEM images. Left and right images are the top surface and the edge of microrods, respectively. In the left images, the periodic arrangement of mesochannels is partially observed. In the right image, mesochannels are oriented parallel along the channel of the PAAM.

The most advantageous point of the vapor infiltration method is that mesoporous metals can be directly deposited onto nonconductive layers in confined spaces. Here, we applied the method to fabricate mesoporous Pt microrods with 100 nm in diameter by using a porous anodic alumina membrane (PAAM) as a hard template. Figure 9a shows the SEM image of the obtained Pt microrods. The Pt microrods were partly arranged in one domain because of the presence of connections between channels arising from PAAM. In the case of the LLC film on a flat substrate, the microparticles in shape are formed because the Pt deposition occurs all over the LLC film (Figure 2). On the other hand, in the case of PAAM, the nucleation sites are limited to only the LLC filled within channels. DMAB vapor molecules reach the exposed surface of the LLC within PAAM channels and dissolve in the hydrophilic region of LLC, and then DMAB molecules infiltrate from the upper side. Therefore, the Pt deposition should proceed in one direction, resulting in the formation of microrods.

The high-magnification SEM image shows a spongelike nanostructure within the microrods (Figure 9b). In some parts, ordered mesochannels are formed (Figure 9c). To the best of our knowledge, such metal-based mesoporous microrods have not been reported so far, though there have been several silica microrods with unique mesoporous structures.[27–31] By utilizing a confined effect, unique mesostructures (e.g., helix, donut, perpendicular alignment) have been generated.[27–31] However, in the present study, mesochannels are randomly oriented and such a confined effect is not observed. Consequently, the new EDIT method combined with vapor infiltration enables facile controls of morphology using a hard matrix like PAAM.

(27) Yamaguchi, A.; Uejo, F.; Yoda, T.; Uchida, T.; Tanamura, Y.; Yamashita, T.; Teramae, N. *Nat. Mater.* **2004**, *3*, 337–341.
(28) Lu, Q.; Gao, F.; Komarneni, S.; Mallouk, T. E. *J. Am. Chem. Soc.* **2004**, *126*, 8650–8651.
(29) Wu, Y. Y.; Cheng, G. S.; Katsov, K.; Sides, S. W.; Wang, J. F.; Tang, J.; Fredrickson, G. H.; Moskovits, M.; Stucky, G. D. *Nat. Mater.* **2004**, *3*, 816–822.
(30) Wang, D. H.; Kou, R.; Yang, Z. L.; He, J. B.; Yang,. Z. Z.; Lu, Y. F. *Chem. Commun.* **2005**, 166–167.
(31) Platschek, B.; Petkov, N.; Bein, T. *Angew. Chem., Int. Ed.* **2006**, *45*, 1134–1138.

Conclusion

Highly ordered mesoporous Pt and Pt-based alloy (Pt−Ru and Pt−Ni) microparticles were deposited from lyotropic liquid crystal (LLC) films including the corresponding metal species via vapor infiltration of a reducing agent of dimethylaminoborane (DMAB). Low-angle XRD measurements and TEM observations proved that the deposited Pt and Pt-based alloy microparticles have 2D hexagonally ordered mesoporous structures. Thus, the method will be widely applicable to the deposition of various metals, binary alloys, and even multicomponent alloys. Our approach using vapor infiltration of a reducing agent enables mesoporous metal microparticles to be created over a large area of substrate. Another advantageous point of the vapor infiltration method is that mesoporous metals can be directly deposited onto nonconductive layers in confined spaces. Mesoporous Pt microrods with 100 nm in diameter were fabricated by using a porous anodic alumina membrane (PAAM) as a hard template. The new EDIT method combined with a vapor infiltration method enables facile controls of morphology by using hard matrix such as PAAM. The macroscopic structural design of mesoporous metals should greatly contribute to future applications such as microsensors, microbatteries, miniaturized devices, and beyond.

Acknowledgment. The authors greatly appreciate the reviewers' helpful comments. The authors acknowledge Prof. Tetsuya Osaka, Dr. Toshiyuki Momma (Waseda University), and Dr. Tokihiko Yokoshima (National Institute of Advanced Industrial Science and Technology, AIST) for critical comments and continuous encouragement. The authors also acknowledge Mr. M. Fuziwara (Kagami Memorial Laboratory for Materials Science and Technology, Waseda University) for TEM observations of mesoporous microparticles. The EDS mapping of mesoporous Pt−Ru alloy microparticles was supported by the "Nanotechnology Support Project" from the Japanese Ministry of Education, Culture, Sports, Science and Technology (MEXT). The present study is supported in part by the Global COE Program "Practical Chemical Wisdom", and the Encouraging Development Strategic Research Centers Program (Super COE) "Establishment of a Consolidated Research Institute for Advanced Science and Medical Care" from MEXT. This work is also supported by the A3 Foresight Program "Synthesis and Structural Resolution of Novel Mesoporous Materials" from the Japan Society for the Promotion of Science (JSPS). This work was supported by a Grant-in-Aid for Scientific Research (19850031) from the Japan Society for the Promotion of Science.

CM701985F